Electronic Supplementary Material (ESI) for Journal of Materials Chemistry C.

In Situ Preparation of Ultrastable and Flexible BA_2PbBr_4 Nanocrystal Films for X-ray Imaging

Yang Li*, Bo Liu, Liang Chen, Shiyi He, Jinliang Liu, Xiang Wang, Naizhe Zhao, Leidang Zhou, Wenyu Shu, Xiaoping Ouyang*

Experimental Section：

Chemicals: Butylammonium Bromid (BABr, 98%) was provided by the: Advanced Election Technology Co,.Ltd. Lead bromide ($PbBr_2$, 99%), dimethylformamide (DMF, 99.9%) and Polymethyl methacrylate (PMMA) were purchased from Aladdin.

Characterization:

Powder X-ray diffraction was performed using an X-ray diffractometer (Bruker, D8 ADVANCE) with Cu Kα radiation (1.54 Å). The optical transmission spectrum was recorded by an UV–vis spectrophotometer (Shimadzu, UV3600 plus). PL spectrum and PLQY were performed on an Edinburgh FLS1000 fluorescence spectrometer excited by the 365 nm xenon lamps. PL decay curve was measured through an Edinburgh FLS1000 fluorescence spectrometer with a 365 nm picosecond pulsed diode laser.

X-ray scintillation measurements

RL spectrum measurements were carried out with an X-ray tube (12 W X-ray source manufactured by Moxtek Inc.) at 30 kV and a spectrometer (Newport 74126). The dose rate was altered by changing the current and calibrated by a dosimeter (RJ32-3602). Decay time was measured by a home-made time-correlated single-photon counting (TCSPC) system which consists of a PMT (ET Enterprises Limited-9815), a microchannel plate (MCP, R3809U-52), a time-to-amplitude converter (TAC, ORTEC 567), a constant-fraction discriminator (ORTEC 935), a timing discriminator (ORTEC 9327), a delay unit (ORTEC, 425) and a computer-controlled multichannel analyzer (Amptek, MCA8000A). The isotope source ^{137}Cs was chosen to be the excitation source. During the decay time measurement, one side of the BA_2PbBr_4 NC@PMMA film is directly coupled to the PMT, which can collect the photons emitted from the scintillator and generate an initial pulse signal.

This initial pulse signal is processed through the subsequent electronics system (a timing discriminator and a delay unit) and triggered by a time-to-amplitude converter as the start signal. Simultaneously, the other side of the BA_2PbBr_4 NC@PMMA film emits the single photons which can be collected by a microchannel plate. The single photon signal produced by the microchannel plate is processed through a constant-fraction discriminator and triggered by the time-to-amplitude converter as a stop signal. The distribution of the time interval between the start signals and stop signal which represent the autocorrelation function of the fluorescence temporal profile can be converted into voltage amplitude by the time-to-amplitude converter. Finally, the voltage amplitude is converted into a digital signal by the multichannel analyzer. The X-ray imaging measurements were performed using a self-build X-ray imaging system which contains an X-ray tube (Anode material: Ag, the radius of an aluminum collimator: 5mm), a mirror and a COMS camera (Tucsen FL-20BW). The X-ray tube, target object and scintillation film are successively placed in the same straight direction. A mirror is used to deflect the light path by 90° to protect the COMS camera from being exposed to X-rays. The X-ray images are captured by the COMS camera. MTF measurement: A sharp-edge X-ray imaging were taken from a 0.5 mm thick tungsten plate, and the X-ray dose rate calibrated by a dosimeter (RJ32-3602) was 825.3 μGyair/s. The edge spread function (ESF) was extracted through processing the X-ray image of the sharp edge, and the corresponding line spread function (LSF) can be obtained by its first derivation. MTF is defined by the Fourier transform of the LSF as follow:

$$MTF(\nu) = F(\mathrm{LSF}(x)) = F(\frac{dESF(x)}{dx})$$

Where ν was the spatial frequency, x was the position of pixel. The above calculations were processed using MATLAB software.

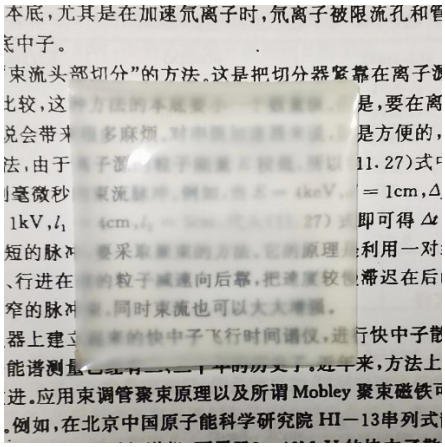

Figure S1 The photograph of the BA_2PbBr_4 NC@PMMA flexible film

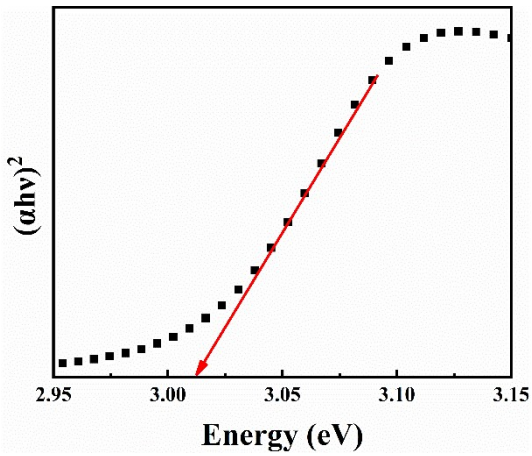

Figure S2 Band gap of BA_2PbBr_4 NC@PMMA flexible film extracted from the Tauc plot.

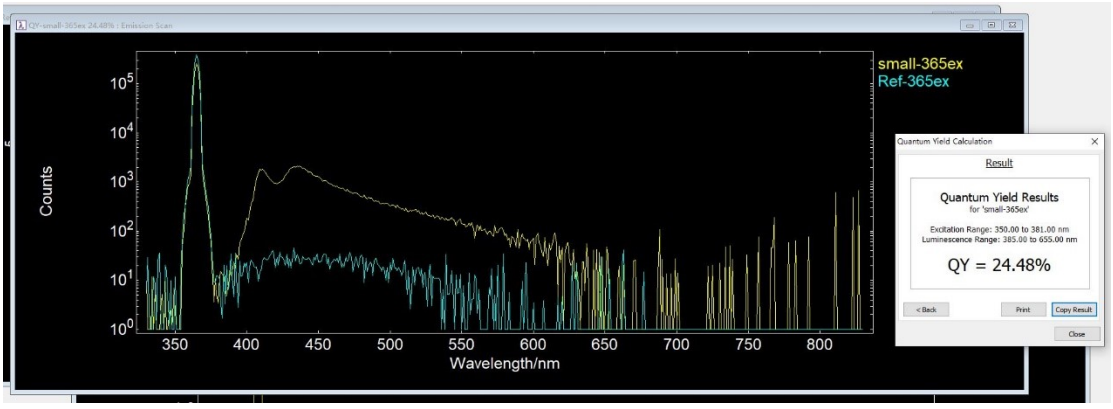

Figure S3 The PLQY curve of BA_2PbBr_4 NC@PMMA film.

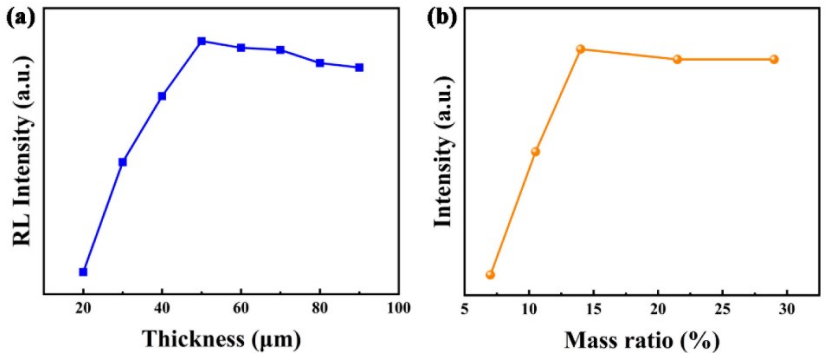

Figure S4 RL intensity of sample with different thickness and mass ratio.

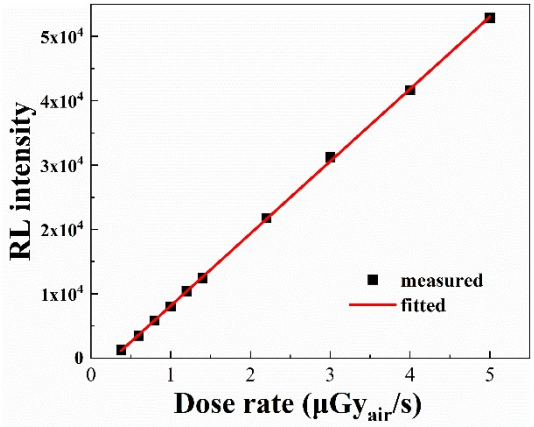

Figure S5 Dose rate-dependent RL spectra of BA_2PbBr_4 NC@PMMA flexible film

Table S1 Comparison of the performances in other flexible scintillators

Material	Detection limit [nGy$_{air}$/s]	Spatial resolution [lp/mm]	PL decay time [ns]	Storage stability [h]	Ref
$CsPbBr_3$/PMMA (40μm)	40.1	8.0	8.25	2520(>80% in water)	1
$CH_3NH_3PbBr_3$ NCs (10μm)	1.6	5.4	63.7	168(>80% in water)	2
$Cs_3Cu_2I_5$ powders/PDMS (100μm)	/	6.8	960	1440 (unchanged in air)	3
$CsPbBr_3$ NCs/AAO (20μm)	/	250	9	4008 (unchanged in air)	4
$(C_{24}H_{20}P)_2MnBr_4$-TPU (115μm)	608	14.5	$3.16*10^5$	4320(unchanged in air)	5
BA2PbBr4 NC@PMMA	588	5.5	2.07	120(>90% in water)	This work

1. B. Wang, J. Peng, X. Yang, W. Cai, H. Xiao, S. Zhao, Q. Lin and Z. Zang, Laser Photonics Rev., 2022, 16, 2100736, DOI: 10.1002/lpor.202100736.

2. Q. Xu, S. Zhou, J. Huang, X. Ouyang, J. Liu, Y. Guo, J. Wang, J. Nie, X. L. Zhang, X. P. Ouyang, W. B. Jia, Mater. Today Phys. 2021, 18, 100390, DOI: 10.1016/j.mtphys.2021.100390.
3. N. Li, Z. Xu, Y. Xiao, Y. Liu, Z. Yang and S. Liu, Adv. Opt. Mater., 2022, 10, 2102232, DOI: 10.1002/adom.202102232.
4. H. H. Li, H. Yang, R. Yuan, Z. X. Sun, Y. L. Yang, J. T. Zhao, Q. L. Li, Z. J. Zhang, Adv. Opt. Mater., 2021, 9, 2101297, DOI: 10.1002/adom.202101297.
5. In Situ Preparation of High-Quality Flexible Manganese Halide Scintillator Films for X-Ray Imaging. K. Xia, P. Ran, W. Wang, J. Yu, G. Xu, K. Wang, X. Pi, Q. He, Y. Yang and J. Pan, Adv. Opt. Mater., 2022, 10, 2201028, DOI: 10.1002/adom.202201028.